

## Effects of mesoscale eddy/wind interactions on biological new production and eddy kinetic energy

Carsten Eden<sup>1</sup> and Heiner Dietze<sup>1</sup>

Received 19 September 2008; revised 12 March 2009; accepted 24 March 2009; published 30 May 2009.

[1] Accounting for ocean currents in the bulk parameterization of the wind stress might represent a physically more plausible way to force an ocean model than ignoring their effect. We show in this study that using the air-sea velocity difference instead of the atmospheric wind in the wind stress formulation dampens both the near-surface eddy activity and the biotic carbon assimilation in a high-resolution model of the North Atlantic. The former is significant, corresponding to a reduction down to 50% in the tropical Atlantic, while in higher latitudes (in agreement with previous results) the reduction of eddy activity is only around 10%. The effect on biotically mediated new production and air-sea carbon fluxes is, on the other hand, minor. New production is reduced by less than 5% on a basin average, while simulated air-sea CO<sub>2</sub> fluxes are barely affected at all. The model results imply that eddy/wind interaction introduced by accounting for ocean currents in the wind stress formulation does not drive any additional (and hitherto unaccounted) nutrient fluxes to the sunlit surface of the subtropical gyre, as was recently proposed in the literature.

**Citation:** Eden, C., and H. Dietze (2009), Effects of mesoscale eddy/wind interactions on biological new production and eddy kinetic energy, *J. Geophys. Res.*, 114, C05023, doi:10.1029/2008JC005129.

### 1. Introduction

[2] Variability of ocean color as observed from space is often correlated with mesoscale physical features (eddies) and therefore suggests a strong physical control of phytoplankton dynamics by mesoscale eddies [e.g., *Doney et al.*, 2003]. This physical control is thought to be linked to mechanisms supplying nutrients to the euphotic zone where they can stimulate growth of phytoplankton. The general idea is that the formation and intensification of cyclonic eddies (CEs) creates low sea level anomalies and upwelling of isopycnal surfaces at depth. This upwelling, often termed eddy pumping, can lift nutrient-rich waters into the euphotic zone thereby fueling new production [e.g., *Jenkins*, 1988; *Falkowski et al.*, 1991; *McGillicuddy and Robinson*, 1997]. Subsequent turbulent vertical mixing, driven by the surface wind stress or surface buoyancy loss, might then transport phytoplankton (as well as nutrients) further up to the surface where it can be observed by satellites.

[3] Less recognized is the physical control of phytoplankton dynamics in anticyclonic eddies (ACEs) where downwelling fed by the convergence of horizontal surface currents during the formation (and intensification) of ACEs can deepen the surface mixed layer. It is clear that this does not drive any transport of new nutrients to the euphotic zone, since it pushes the nutrient-depleted surface waters into the aphotic zone. Furthermore, the deepening of the surface mixed layer in ACEs can reduce the temporally averaged light, experienced by phytoplankton cells dis-

persed in the surface mixed layer [e.g., *Tilburg et al.*, 2002], thus inhibiting phytoplankton growth. Hence, because of the differing physical frameworks, cyclonic eddies should be more productive and might therefore accommodate higher phytoplankton concentrations than their anticyclonic counterparts.

[4] In the North Atlantic (among other locations), however, there are exceptions to the above rule. Phytoplankton concentrations in ACEs which are significantly higher than those found in their cyclonic counterparts or ambient surface water, e.g., have been documented by *Olson* [1986] and *Martin and Richards* [2001]. One mechanism potentially driving at least some of these anomalous high phytoplankton concentrations observed in ACEs was, to our knowledge, first described by *Dewar and Flierl* [1987], put forward by *Martin and Richards* [2001] and *McGillicuddy et al.* [2007], and is coined eddy/wind interaction: A spatially uniform wind blowing over an ACE results in a differential wind stress on diametrically opposite sides of the eddy because of the relative air-sea velocity being different on either side. Estimates of the related Ekman pumping (proportional to the curl of the wind stress) yield an upward vertical velocity (downward in case of an CE), which is of the order of 0.5 m d<sup>-1</sup> for typical ACEs and wind speeds.

[5] Recently, *McGillicuddy et al.* [2007] and *Ledwell et al.* [2008] discussed the upwelling induced by eddy/wind interaction in an anticyclonic mode-water eddy on the basis of a comprehensive set of observations which includes a sulfur hexafluoride tracer release experiment. They concluded that there was indeed significant upward nutrient transport fueling phytoplankton growth and subsequent export of particulate organic material sinking out of the

<sup>1</sup>IFM-GEOMAR, Kiel, Germany.

surface ocean due to the eddy/wind interaction. It was proposed by *McGillicuddy et al.* [2007] and *Ledwell et al.* [2008] that the eddy/wind interaction and the related vertical velocities might help to resolve an apparent, long-standing discrepancy between nutrient supply to [Lewis et al., 1986] and oxygen consumption below [Jenkins, 1982] the euphotic zone of the subtropical gyre.

[6] On the other hand, the relevance of the eddy/wind interaction has been questioned by *Mahadevan et al.* [2008], since scaling arguments, also put forward by *Martin and Richards* [2001], suggest that the vertical velocities associated with the eddy/wind interaction are orders of magnitude smaller than other (ageostrophic) vertical velocities associated with mesoscale and submesoscale eddies. Increased magnitudes of vertical velocities due to (submesoscale) mesoscale variability were discussed for instance by *Giordani et al.* [2006] and *Legal et al.* [2007] using observational results and by *Haine and Marshall* [1998], *Mahadevan and Tandon* [2006], and *Capet et al.* [2008] using model results. Furthermore, *Martin et al.* [2001], *Lévy et al.* [2001], *Lévy* [2003], and *Mahadevan and Archer* [2000] demonstrated the potential of increased vertical velocities related to (submesoscale) mesoscale eddy variability and consequently higher biotic production.

[7] In this study, we focus on quantifying the effect of eddy/wind interaction on annual new production and air-sea carbon fluxes in a realistic basin-scale model. To revise previous large-scale model-based estimates [e.g., *Oschlies and Garçon*, 1998; *Oschlies*, 2002b; *McGillicuddy et al.*, 2003] which neglected the nutrient supply to surface waters induced by the eddy/wind interaction, we discuss two versions of a coupled ecosystem-ocean circulation model with mesoscale eddy-permitting resolution of the North Atlantic. One version includes the feedback of ocean surface currents on the wind stress forcing the surface ocean, while the other version ignores that feedback.

[8] The second focus of this study is to understand the effect of the revised wind stress formulation and the eddy/wind interaction on the simulation of the mean circulation and, in particular, on the mesoscale eddy activity. *Pacanowski* [1987] first discussed the effect of including the ocean currents in the formulation of the wind stress forcing a coarse resolution model of the tropical Atlantic ocean and reported some improvements in the simulation, apparently resulting from the more realistic forcing function. Nevertheless, this effect has been ignored in ocean modeling until recently. The importance of including ocean currents in the formulation of the wind stress was revisited by *Duhaut and Straub* [2006], *Zhai and Greatbatch* [2007], and *Xu and Scott* [2008] with respect to the mechanical energy input by the wind stress into the ocean. These studies reported a significant reduction on the total energy input by the revised wind stress formulation and also a damping effect on the EKE by about 10% by the eddy/wind interaction. While *Zhai and Greatbatch* [2007] considered the subpolar region of the North Atlantic only, we extend these studies to a basin-wide estimate of the damping effect of the eddy/wind interaction on EKE and to a detailed analysis of the causes of the EKE decrease.

[9] In the following section we describe our main tool, the coupled ecosystem-ocean circulation model. In section 3.1, we discuss the effect of taking into account surface ocean

currents in the parameterization of the wind stress driving the ocean model on the wind stress itself. The sections 3.2, 3.3, and 3.4 present the impact of circulation/wind stress interaction on the circulation itself. The associated biotic responses, as represented by the ecosystem model, are discussed in sections 3.5 and 3.6. The last section summarizes our findings.

## 2. Model Configuration and Experiments

[10] We use a general circulation model of the North Atlantic Ocean with a nominal horizontal resolution of  $1/12^\circ$  which ranges from about  $5 \times 5$  km at high latitudes to  $10 \times 10$  km at low latitudes. The vertical grid comprises 45 levels with 10 m thickness near the surface increasing downward to 250 m. The model domain extends from  $20^\circ\text{S}$  to  $70^\circ\text{N}$  with an open boundary formulation following *Stevens* [1990] at the northern and southern boundary and a restoring zone within the Mediterranean Sea. A simple nitrogen-based four-compartment ecosystem (so-called NPZD) model is coupled online to the ocean circulation model. There is no impact of biotic processes on the circulation via, for example, absorption of solar radiation modified by modeled phytoplankton concentrations. In case of inflow conditions at the boundaries, i.e., when the velocity at the open boundaries, as calculated by the formulation by *Stevens* [1990], is directed into the model domain, temperature, salinity and nitrate are prescribed using a combined climatology from *Boyer and Levitus* [1997] and *Levitus and Boyer* [1994]. The same applies for the restoring zone and initial conditions. Phytoplankton and zooplankton are initialized with small concentrations at the surface corresponding to a nitrogen equivalent of  $0.05 \text{ mmol m}^{-3}$ .

[11] The coupled ecosystem-ocean circulation model is identical to the one used by, e.g., *Eden* [2006] and *Eden and Oschlies* [2006] except for the following modifications:

[12] 1. Vertical mixing of momentum, temperature, salinity and passive (biogeochemical) tracers near the surface is parameterized with a turbulent kinetic energy (TKE) scheme following *Gaspar et al.* [1990].

[13] 2. Solar radiation penetrates into the water column, and its absorption is parameterized by the analytical formula of *Paulson and Simpson* [1977] for clear ocean water (type I after *Jerlov* [1976]).

[14] 3. Modified surface forcing: All integrations discussed here are preceded by a 30 year spin-up forced with a monthly mean climatology at the surface. More specifically, the climatological surface forcing is that from a 3 year analysis of the T94 version of the ECMWF weather forecast model [Barnier et al., 1995]. The surface heat flux formulation is a Haney-type relaxation [Barnier et al., 1995] while sea surface salinity (SSS) is simply restored to monthly mean SSS from the initial conditions with a timescale of 30 days. The input of TKE by surface winds and associated breaking waves which poses the boundary condition for the vertical mixing scheme of *Gaspar et al.* [1990] is parameterized by the friction velocity  $u^*$  calculated with the monthly mean climatological wind stress [Barnier et al., 1995].

[15] The ecosystem model is coupled to the ocean circulation model during the latter 20 years of the spin-up to allow for an adjustment of the nutrient field within the main

thermocline and above. Simulated dissolved inorganic carbon (DIC) is coupled to nitrate using a constant carbon to nitrate ratio in each compartment of the ecosystem model [Eden and Oschlies, 2006]. Surface boundary and initial conditions for DIC are also identical to Eden and Oschlies's [2006], i.e., (preindustrial) air-sea carbon fluxes are calculated using oceanic surface  $p\text{CO}_2$  as a function of simulated dissolved inorganic carbon, temperature, salinity and alkalinity, where alkalinity is given as a function of salinity [Eden and Oschlies, 2006].

[16] We discuss two subsequent sensitivity integrations following the spin-up phase (as described in detail below). Both sensitivity experiments are driven by daily mean wind stress, surface heat flux and friction velocity  $u^*$  derived from the daily analysis (2001–2006) of the high-resolution (T511, i.e., about  $40 \times 40$  km horizontal resolution) ECMWF weather forecast model [Eden and Jung, 2006]. All other components forcing the model, including the relaxation of SST toward the monthly mean climatology, are identical to the setup during the spin-up phase.

[17] The two sensitivity integrations differ in the formulation of the surface wind stress. The standard formulation (as applied by, e.g., Smith *et al.* [2000], Eden and Böning [2002], Oschlies [2002b], and McGillicuddy *et al.* [2003]) for wind stress forcing an ocean model, given by

$$\tau_{std} = \rho_a c_D |\mathbf{u}_a| \mathbf{u}_a \quad (1)$$

(with wind stress seen by the ocean's surface  $\tau_{std}$ , density of air  $\rho_a$ , atmospheric wind velocity  $\mathbf{u}_a$ , dimensionless drag coefficient  $c_D$ ) does not include any feedback of ocean surface currents on the wind stress driving the ocean. In the present study,  $\tau_{std}$  stems from the low-resolution ECMWF model during the spin-up phase and from the T511 ECMWF model in the subsequent integrations. The ocean model forced with the standard formulation of the wind stress will be called the reference experiment.

[18] The experiment WINDFEED corresponds to an integration with a revised, more plausible, formulation for the wind stress,  $\tau_{rev}$ , which takes the feedback of ocean surface currents on the wind stress into account [Large and Yeager, 2004]

$$\tau_{rev} = \rho_a c_D |\mathbf{u}_a - \mathbf{u}_o| (\mathbf{u}_a - \mathbf{u}_o), \quad (2)$$

where  $\mathbf{u}_o$  denotes the modeled horizontal ocean currents. The atmospheric wind  $\mathbf{u}_a$  is derived from the same surface forcing  $\tau_{std}$  applied in the reference experiment by assuming a constant drag coefficient of  $c_D = 1.2 \times 10^{-3}$ . Hence, the only difference between the reference experiment and WINDFEED is the feedback of ocean currents on wind stress in the model integrations from 2001 to 2006. Both integrations covering the period from 2001 to 2006 are forced with the identical high-resolution surface forcing from the T511 ECMWF model.

### 3. Results

[19] In this section, we first discuss in detail the changes in the circulation due to the different formulation of the wind stress and its possible causes. We refer those readers which are more interested in the biogeochemical aspects of

the present study, i.e., the impact of the eddy/wind interaction on standing stocks of phytoplankton, associated new production and air-sea carbon fluxes, directly to sections 3.5 and 3.6.

#### 3.1. Wind Stress Curl

[20] The large-scale structure of the annual mean wind stress curl ( $\mathbf{k} \cdot \nabla \times \boldsymbol{\tau}$ ) is similar in the reference experiment and WINDFEED (Figure 1): Negative (positive) wind stress curl over the subtropical (subpolar) gyre driving downward (upward) velocities below the surface Ekman layer and southward (northward) Sverdrup transport which can explain much of the large-scale structure of the circulation in the North Atlantic. A previous study by Eden and Jung [2006] showed that these large-scale features in the wind stress curl are similar to the wind stress curl derived from the low-resolution ECMWF model [Barnier *et al.*, 1995] which drives the model during the shared spin-up phase while small differences in magnitudes and structure of the large-scale features can be attributed to interannual variability of the atmospheric circulation.

[21] Small-scale features in Figures 1a and 1b, however, differ as a consequence of the ocean currents altering the wind stress. Most prominent is the Gulf Stream/North Atlantic Current (NAC) system extending downstream into the subpolar gyre where mesoscale structures related to the oceanic eddy field are clearly revealed in the experiment WINDFEED while this does not hold for the reference experiment. Differences are also evident in the western boundary currents, the Gulf stream itself and the North Brazil Current.

[22] Also shown in Figure 1c is the curl of the wind stress derived from the QuikSCAT microwave scatterometer, which is a satellite-mounted radar that transmits microwave pulses from space down to the Earth's surface and measures the backscatter. For the open ocean, the backscatter is related to surface waves, which are in turn related to the stress between ocean and atmosphere. The gridded wind stress data product at 25 km resolution twice per day is provided by the Centre ERS d'Archivage et de Traitement (CERSAT), at IFREMER, Plouzané, France.

[23] The stress derived from the QuikSCAT scatterometer data includes at least some of the effects of ocean currents, a fact that can be seen, for instance, off the east coast of North America south of about  $35^\circ\text{N}$  where a positive wind stress curl anomaly in QuikSCAT is spatially correlated with the location of the Gulf stream. Moreover, much of the fine-scale structures in wind stress curl from QuikSCAT are reproduced in the experiment WINDFEED rather than in the reference experiment, which, in reverse, is an indication that a lot of the mesoscale features in the QuikSCAT wind stress curl is caused by a feedback of ocean surface currents on wind stress. Here, we conclude that considering the effect of ocean currents clearly improves the model simulation in terms of the realism of the forcing, but note the subtleties in using QuikSCAT data directly to force ocean models as discussed recently by Xu and Scott [2008].

[24] The T511 ECMWF model, which is used in deriving the wind stress for both the reference and WINDFEED experiments, assimilates scatterometer winds (from June 1996 onward ERS-2 data, from January 2002 onward QuikSCAT data, from June 2007 onward ASCAT on

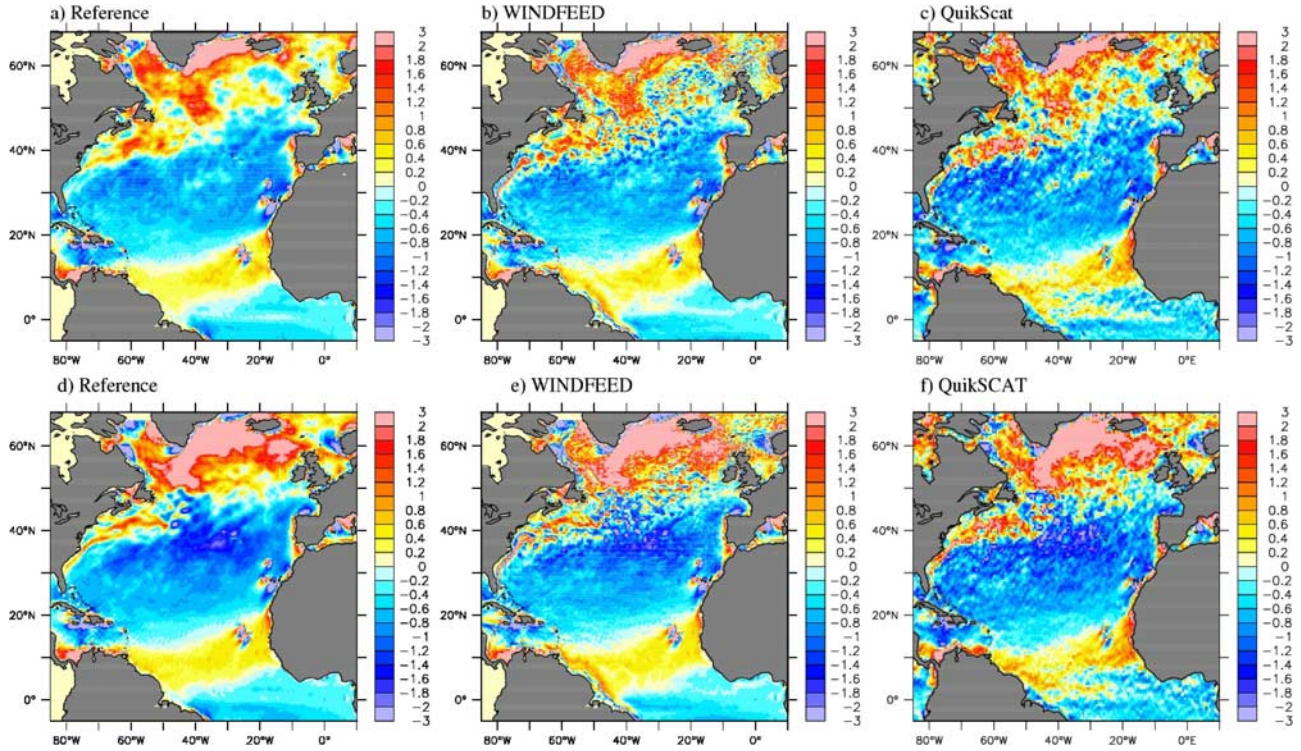


**Figure 1.** Wind stress curl in  $10^{-7} \text{ N m}^{-3}$  averaged over the years (a, b, c) 2001 and (d, e, f) 2002 and box averaged over  $1/3^\circ \times 1/3^\circ$  prior to plotting. Figures 1a and 1d refer to the reference experiment, and Figures 1b and 1e refer to the WINDFEED experiment. Figures 1c and 1f show QuikSCAT observations.

MetOp-A, according to T. Jung and H. Hersbach (personal communication, 2008)). This is problematic since wind stress, derived from scatterometer data, implicitly carries information about the real-world ocean currents which leads to subtleties when applied to ocean models where modeled currents will, inevitably, deviate from reality [Xu and Scott, 2008]. In 2001, only ERS-2 scatterometer winds have been assimilated in the ECMWF model and their impact seems to be weak since the imprint of the Gulf Stream can hardly be seen in Figure 1a. This changes slightly in 2002 when assimilation of QuikSCAT data in the ECMWF model system begins and positive wind stress curl anomalies off

the east coast of Florida, spatially correlated with the position of the Gulf stream, start to show up in the reference experiment (Figures 1e and 1f). The amplitude of this effect is however weak when compared to the satellite observations and in particular when compared with experiment WINDFEED. The following years are alike 2002 in this respect.

### 3.2. Mean and Eddy Kinetic Energy

[25] Figure 2 shows the near-surface mean kinetic energy (MKE,  $\frac{(\bar{u}_0)^2}{2}$  where the overbar denotes an average in time) in the reference experiment, WINDFEED and the difference

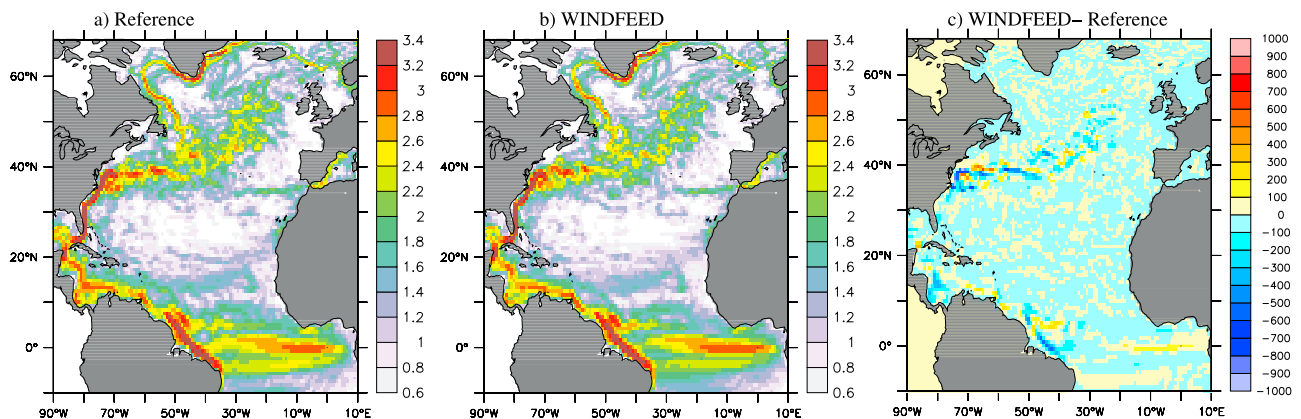


**Figure 2.** Mean kinetic energy (MKE) (average of the upper 50 m) in the year 2001 in  $\log_{10}(\text{MKE cm}^{-2} \text{ s}^{-2})$  for (a) the reference experiment, (b) WINDFEED, and (c) difference (WINDFEED – reference experiment) in  $\text{cm}^2 \text{ s}^{-2}$ .

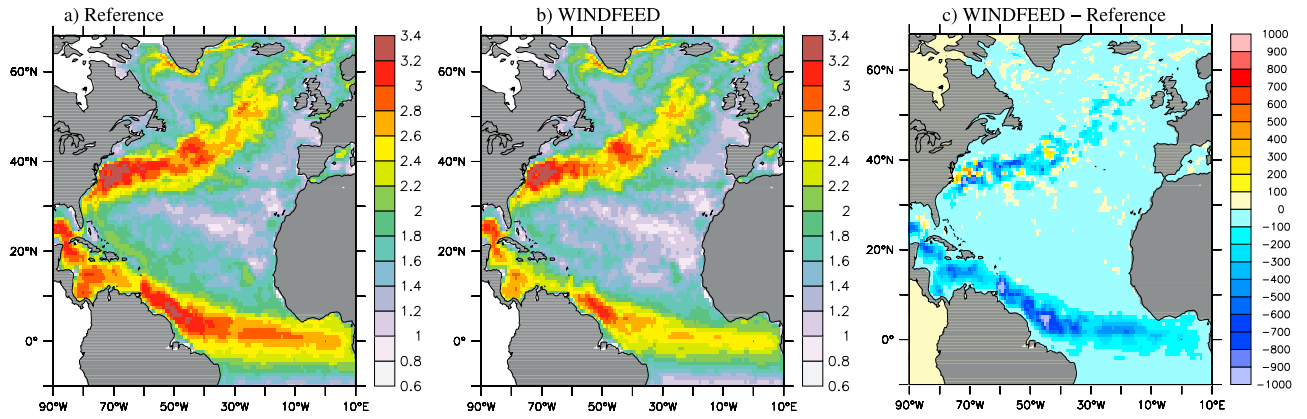


**Figure 3.** Eddy kinetic energy (EKE) (average of the upper 50 m) in 2001 in  $\log_{10}(\text{EKE cm}^{-2} \text{ s}^{-2})$  for (a) the reference experiment, (b) WINDFEED, and (c) difference (WINDFEED – reference experiment) in  $\text{cm}^2 \text{ s}^{-2}$ .

between both for the year 2001. Besides a small eddy signal in the Gulf Stream/North Atlantic Current system, there are only minor systematic changes in the mean circulation of the model. This applies for the subsequent years as well (Figure 4). The only systematic effect of including the ocean currents in the formulation of the wind stress forcing is a reduction of the mean South Equatorial Current (SEC) and Equatorial Under Current (EUC) in the tropical Atlantic Ocean, coming along with a slight decrease of the depth level of the EUC (not shown) and a decrease of the equatorial upwelling as discussed below. This effect is consistent with the results of Pacanowski [1987], who found a similar response in a non-eddy-resolving model of the tropical Atlantic and a better agreement between their model results and situ current meter observations after including the effect of ocean currents on wind stress in their model.

[26] The near-surface eddy kinetic energy ( $\text{EKE}, \frac{\overline{u'^2}}{2}$  where the prime denotes deviation from a seasonal mean), on the other hand, is significantly different in the reference experiment and WINDFEED. Figure 3 shows the EKE in both experiments for the year 2001. Note that we have estimated the EKE (and the other correlations discussed in sections 3.3 and 3.4) as deviations from the seasonal mean of velocity (and other quantities) to exclude the seasonal cycle from the analysis. Note also that we have used the individual seasonal means for 2001–2006 in both experiments to obtain the perturbation quantities. Clearly, the effect of including the ocean currents in the wind stress is to damp EKE. This effect is large in the tropical Atlantic, decreases toward higher latitudes and has a second peak where the Gulf Stream separates from the American coast. The subsequent years are similar with respect to the reduction of EKE (Figure 4).

### 3.3. Eddy Kinetic Energy Budget

[27] To identify the mechanisms behind the large differences in the eddy activity of the reference experiment and WINDFEED, we consider the budget of EKE,  $\bar{e} = \frac{\overline{u'^2}}{2}$  as given by the standard Reynolds averaging procedure

$$\partial_t \bar{e} + \nabla_h \cdot (\overline{u_o e} + \overline{u'_o p'}) + \partial_z \overline{w' p'} = \bar{S} + \overline{b' w'} - \varepsilon, \quad (3)$$

where  $p'$  denotes pressure fluctuations,  $b'$  buoyancy fluctuations and  $w'$  fluctuations of the vertical velocity. The EKE budget equation (3) is derived by taking the average of the scalar product of the horizontal momentum perturbation  $\mathbf{u}'_o$  with the horizontal momentum budget of the primitive equations. The terms on the l.h.s of equation (3) describe changes of EKE ( $\partial_t \bar{e}$ ) due to advective and radiative processes which cancel out in the domain integral while the terms on the r.h.s of equation (3) can be interpreted as production of EKE due to lateral shear,  $\bar{S} = -\overline{\mathbf{u}'_o \mathbf{u}'_o} \cdot \nabla \overline{\mathbf{u}_o}$ , production by baroclinic instability,  $\overline{b' w'}$ , and dissipative processes,  $\varepsilon$  [Beckmann et al., 1994]. Note that  $\varepsilon$  includes also the surface forcing of EKE arising from the wind acting on the ocean,  $\overline{\mathbf{u}'_o \cdot \boldsymbol{\tau}'}$ .

[28] We define two pathways via which changes in the EKE can be affected by changes in the parameterization of the wind stress, a direct one and an indirect one. The indirect pathway refers to changes in wind stress acting on the ocean, driving changes in the mean circulation and mean available potential energy which in turn will affect the EKE production terms  $\bar{S}$  and  $\overline{b' w'}$ . The direct pathway, on the other hand, is the drag effect by a modified wind stress on the EKE budget (entering equation (3) via  $\varepsilon$ ), as explained later.

[29] First we quantify the indirect pathway: Figures 4c and 4d show the zonal averages of the production terms of EKE in the reference experiment and WINDFEED. While differences in  $\overline{b' w'}$  are only small, the production terms  $\bar{S}$  show similar differences as the EKE itself in the two experiments. The reduction of  $\bar{S}$  in experiment WINDFEED relative to the reference is both due to a reduction in the lateral shear of the mean flow,  $\nabla \overline{\mathbf{u}_o}$ , and a decreased magnitude of the tensor  $\overline{\mathbf{u}'_o \mathbf{u}'_o}$ . The decrease in lateral shear is in particular large in the tropical Atlantic.

[30] Second, we continue with a quantification of the direct drag effect (of the revised wind stress formulation) on the total kinetic energy of the ocean and in particular to the EKE following Duhaut and Straub [2006] and Zhai and Greatbatch [2007]. The work  $P$  done by the wind stress  $\boldsymbol{\tau}$  is forcing the ocean's total kinetic energy  $\mathbf{u}_o^2/2$  and is given by

$$\rho_o P = \boldsymbol{\tau} \cdot \mathbf{u}_o = \rho_a c_D |\mathbf{u}_a - \mathbf{u}_o| (\mathbf{u}_a - \mathbf{u}_o) \cdot \mathbf{u}_o, \quad (4)$$

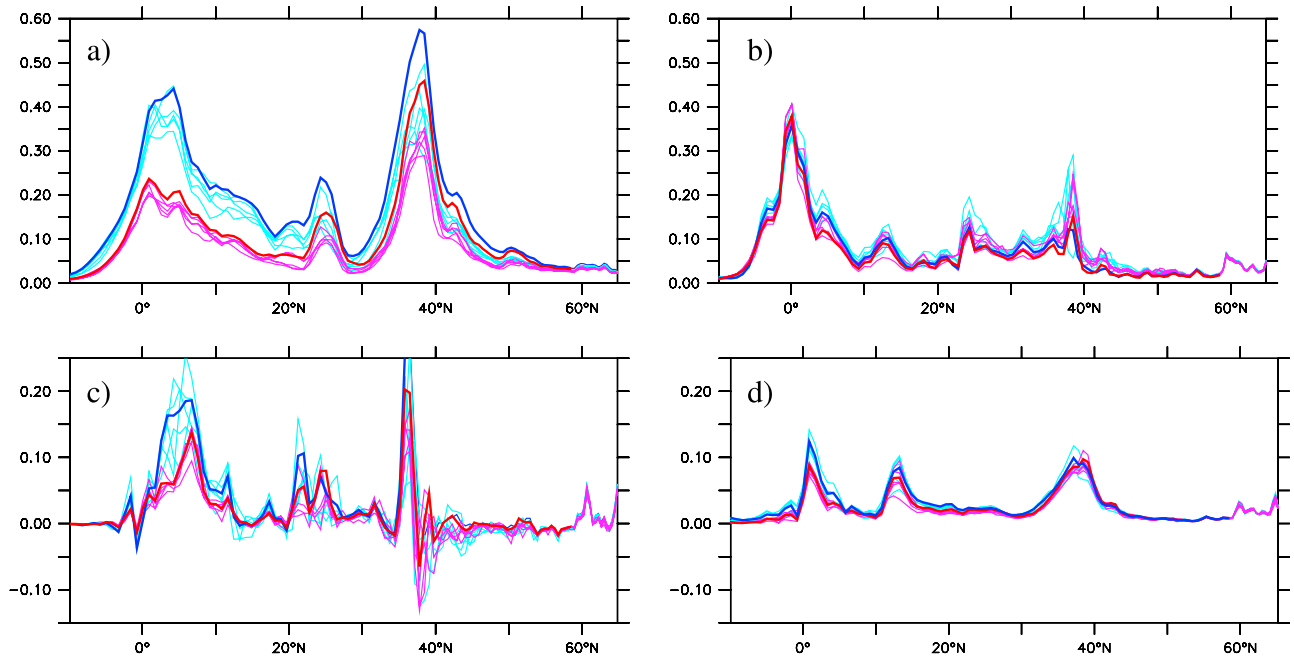


**Figure 4.** Annual mean, zonally integrated (a) EKE and (b) MKE for the reference experiment (blue lines) and WINDFEED (red lines) (average of the upper 50 m) in  $10^6 \text{ m}^3 \text{ s}^{-2}$  for the years 2001 to 2005 and total average over these years (bold lines). Also shown are zonal integrals of EKE production due to (c) lateral shear of the mean current ( $\bar{S} = -\mathbf{u}'_o \mathbf{u}'_o \cdot \nabla \bar{\mathbf{u}}_o$ ) and (d) baroclinic instability ( $\bar{b}'w'$ ) in  $\text{m}^2 \text{ s}^{-3}$  (average of the upper 50 m) in the same color coding.

where  $\rho_0$  denotes the reference density of sea water,  $\rho_a$  the density of air,  $c_D$  the drag coefficient and  $\mathbf{u}_a$  and  $\mathbf{u}_o$  the velocity of air and sea water, respectively. The difference in wind work due to the formulations for  $\tau$  is (assuming identical  $\mathbf{u}_o$  in both cases)

$$\rho_0(P_{rev} - P_{std}) = -\rho_a c_D |\mathbf{u}_a - \mathbf{u}_o| |\mathbf{u}_o|^2 - \rho_a c_D (|\mathbf{u}_a| - |\mathbf{u}_a - \mathbf{u}_o|) \mathbf{u}_a \cdot \mathbf{u}_o, \quad (5)$$

where  $P_{rev}$  and  $P_{std}$  denote the wind work in the revised and the standard wind stress formulation, respectively. The first term is negative and is believed to dominate [Duhaut and Straub, 2006; Zhai and Greatbatch, 2007]. Since for  $\mathbf{u}_a \cdot \mathbf{u}_o > 0$ , we find  $|\mathbf{u}_a| - |\mathbf{u}_a - \mathbf{u}_o| > 0$  and vice versa, the second term is also sign definite and the effect of the revised formulation of wind stress is to remove energy, i.e., to apply a surface drag on the circulation. However, note that in general  $\mathbf{u}_o$  will change by applying a different wind stress, but it is reasonable to assume that the change will not reverse the sign of the effect. Another reasonable assumption is that the difference in atmospheric winds and oceanic currents does not significantly affect the amplitude of the wind stress since surface winds are usually at least an order of magnitude faster than surface currents, i.e.,  $|\mathbf{u}_a - \mathbf{u}_o| \approx |\mathbf{u}_a|$  such that the difference in the wind work  $P$  between both formulation simply becomes to leading order

$$\rho_0(P_{rev} - P_{std}) \approx -\rho_a c_D |\mathbf{u}_a| |\mathbf{u}_o|^2. \quad (6)$$

The difference in wind work for the eddy kinetic energy,  $\frac{\overline{u_o'^2}}{2}$  is thus given by

$$\rho_0(P'_{rev} - P'_{std}) \approx -\rho_a c_D |\bar{\mathbf{u}}_a| \overline{u_o'^2}, \quad (7)$$

neglecting, for simplicity, any correlation between wind speed and ocean current fluctuations which should be similar in both formulations of  $\tau$ . The perturbation velocity  $\mathbf{u}'$  is again a deviation from the seasonal mean as throughout this study.

[31] To conclude with a quantitative comparison of the direct and indirect effect of the revised wind stress parameterization, Figure 5 shows zonally integrated EKE production terms within the upper 50 m of the ocean which reveals: The direct drag by the eddy/wind interaction as given by equation (7), is predominantly driving the reduction of the EKE, while the indirect effect of a reduction in  $\bar{S}$  due to the reduced strength of EKE and lateral shear of the mean flow is of secondary importance.

### 3.4. Equatorial Upwelling

[32] Figures 6a and 6d shows the Eulerian mean meridional stream function defined by

$$\partial_z \psi_m(y, z) = \int \bar{v}(x, y, z) dx \quad (8)$$

for the reference experiment and WINDFEED.  $v$  denotes meridional velocity, and  $\bar{v}$  the temporal average of  $v$  (over year 2001). The zonal integral is taken over the whole basin.

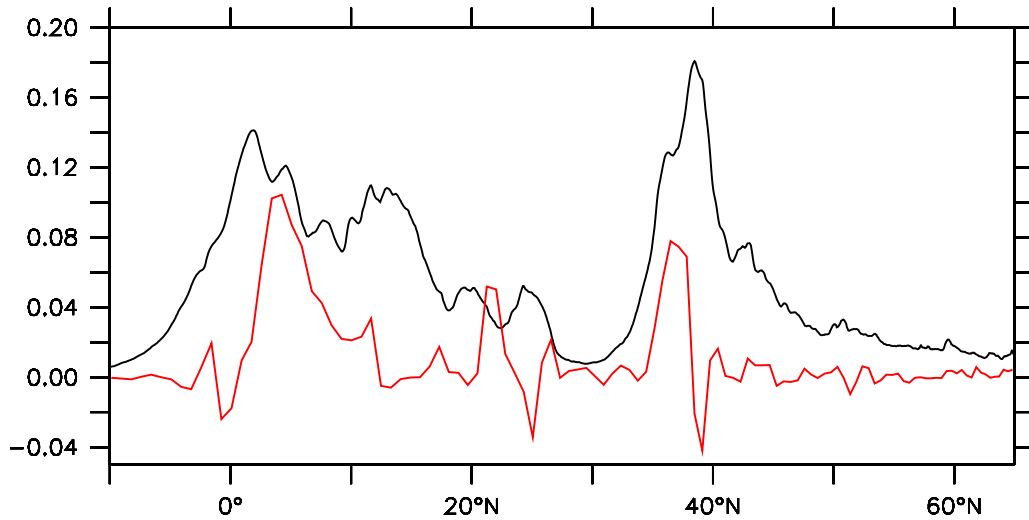


**Figure 5.** Estimate of the drag effect by the eddy/wind interaction on the EKE of the upper 50 m of the ocean, i.e.,  $c_d \rho_a / \rho_0 |\bar{\mathbf{u}}_a| \mathbf{u}'_o{}^2 / 50$  m as given by equation (7) for the year 2001 (black) and difference (reference experiment – WINDFEED) in EKE production due to lateral shear,  $\bar{S} = -\bar{\mathbf{u}}'_o \cdot \nabla \bar{\mathbf{u}}_o$ , averaged over the upper 50 m (red) and years 2001 to 2005 in  $\text{m}^2 \text{s}^{-3}$ . See text for more details.

In both experiments,  $\psi_m$  shows upwelling at the equator of more than 20 Sv, which is, however, reduced by about 4 Sv at 40 m in the experiment WINDFEED which includes the effect of ocean currents in the wind stress formulation. This reduction in the mean upwelling was also described by Pacanowski [1987] in a non-eddy-resolving model and comes along with a decrease in the strength of the mean South Equatorial Current (SEC) and Equatorial Under Current (EUC) and a slight decrease of the depth level of the EUC (not shown).

[33] The reduction in the Eulerian mean equatorial upwelling is related to the modified, reduced, wind stress over the equator: Figure 7 shows the wind stress in 2001 for the reference experiment and the difference between the wind stress in experiment WINDFEED and the reference experiment. The changes in wind stress are largest in the tropical Atlantic. North of the equator between 0° and the intertropical convergence zone at about 2°N the reduction relative to the reference experiment peaks at around 10%. This reduced, northwestward wind stress, leads to a reduced off-

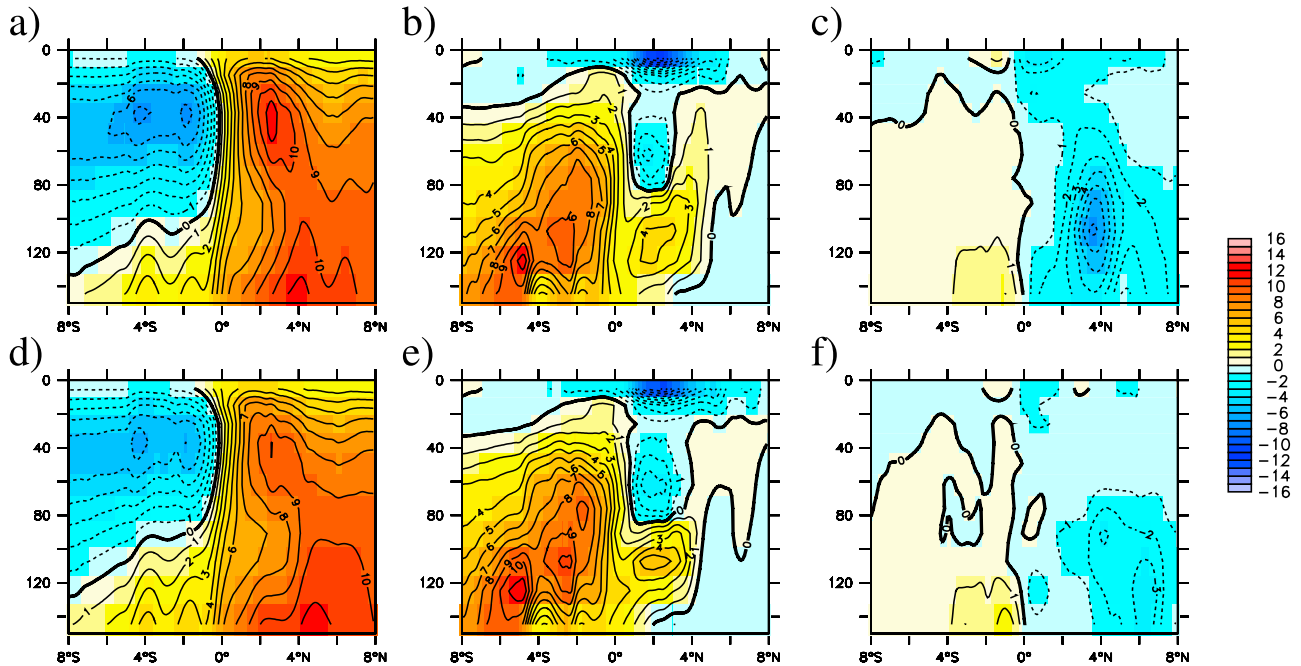


**Figure 6.** (a, d) Eulerian mean meridional overturning stream function  $\psi_m$  in Sv for the reference experiment (Figure 6a) and WINDFEED (Figure 6d). (b, e) Standing eddy contribution  $S$  for the reference experiment (Figure 6b) and WINDFEED (Figure 6e). (c, f) Transient eddy contribution  $T$  for the reference experiment (Figure 6c) and WINDFEED (Figure 6f).

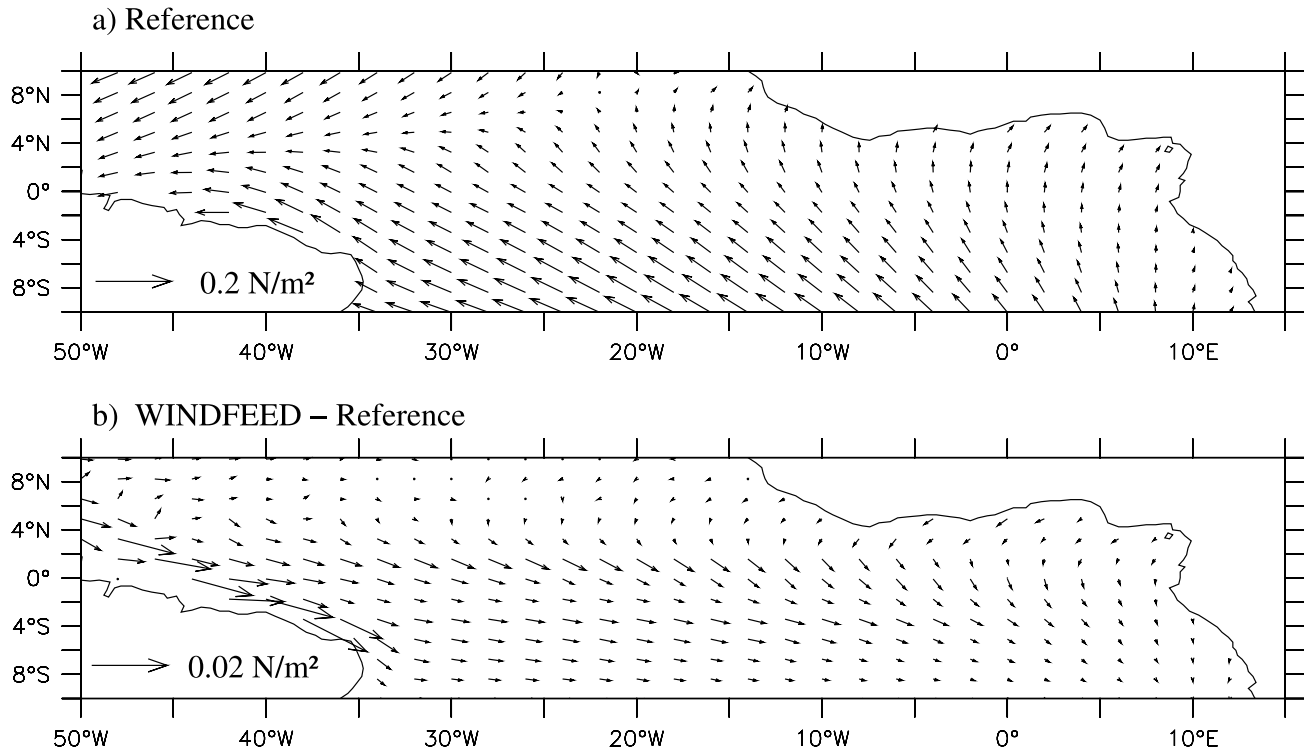


**Figure 7.** (a) Annual mean wind stress in  $\text{N m}^{-2}$  in the reference experiment for year 2001. (b) Same as Figure 7a but for difference in wind stress between the experiments (reference experiment – WINDFEED).

equatorial Ekman transport and thus to a reduced equatorial upwelling. An additional but smaller contribution suppressing the off-equatorial Ekman transport comes from a reduction of the westward component of the wind stress south of the equator.

[34] Drawing conclusions from the Eulerian mean stream function  $\psi_m$  alone is problematic since the actual advective pathways of mean tracer distributions might well be changed because of eddy effects. In the Transformed Eulerian Mean (TEM) framework of *Andrews et al.* [1987], the effect of standing or transient eddy signals is interpreted as an additional advection velocity for the tracer under consideration, which can for instance lead to a significant eddy-driven upwelling. In the oceanographic community, this eddy-induced advection is often called the bolus velocity [*Gent and McWilliams, 1990*]. The TEM framework allows the formulation of a residual stream function,  $\psi$ , which describes the net effect of Eulerian mean advection velocity and eddy-induced advection velocity on the mean tracer. That means that  $\psi$  accounts for the mean advection  $\psi_m$ , effects of standing eddies ( $S$ ) and transient (mesoscale) eddies ( $T$ ). It is given by

$$\psi = \psi_m + S + T \quad \text{with} \quad S = \widehat{\bar{b}^* \bar{v}^*} L / \partial_z \hat{b} \\ \text{and} \quad T = \widehat{\bar{b}' \bar{v}'} L / \partial_z \hat{b}, \quad (9)$$

where  $b$  denotes buoyancy (buoyancy  $b = -g/\rho_0\rho$  is calculated using potential density  $\rho$  referenced to the surface, where  $g$  denotes acceleration of gravity and  $\rho_0$  a fixed reference density according to the Boussinesq

approximation),  $\hat{v}$  ( $\hat{b}$ , etc.) the zonal average of  $v$  ( $b$ , etc.),  $v^*$  ( $v'$ ) deviations from the zonal (temporal) average of  $v$ , and  $L = L(y, z)$  the zonal length of the ocean. Note that the temporal fluctuations exclude again the seasonal cycle. Figure 6 shows the contributions by the standing and transient eddies for the reference experiment and WINDFEED. While  $S$  is similar in both experiments, the downwelling driven by transient mesoscale eddies is reduced in WINDFEED below 50 m at around 4°N. Note that the amplitude of this reduction is less than the difference in the Eulerian mean stream function. Hence, for the actual advective pathways of mean tracer distributions, we conclude that the upwelling at the equator is significantly reduced if the effect of ocean currents in the wind stress formulation is taken into account.

### 3.5. Phytoplankton Standing Stocks

[35] Figure 8 shows the vertically integrated annual mean phytoplankton standing stock in 2001 for the reference experiment and WINDFEED in carbon units (converted from our nitrogen-based ecosystem model with a fixed Redfield carbon ( $C$ ) to nitrate ( $N$ ) ratio of  $C/N = 6.6$ ). Two maxima in the simulated phytoplankton concentration of the North Atlantic show up, one is located north of the oligotrophic subtropical gyre coinciding roughly with the region covered by the Gulf Stream/NAC system and the other one is located in the equatorial upwelling region. Smaller phytoplankton-rich regions are located in the coastal upwelling regions off the coast of west Africa and the coast of Brazil north of the equator. Note that amplitude and spatial distribution of phytoplankton standing stocks are

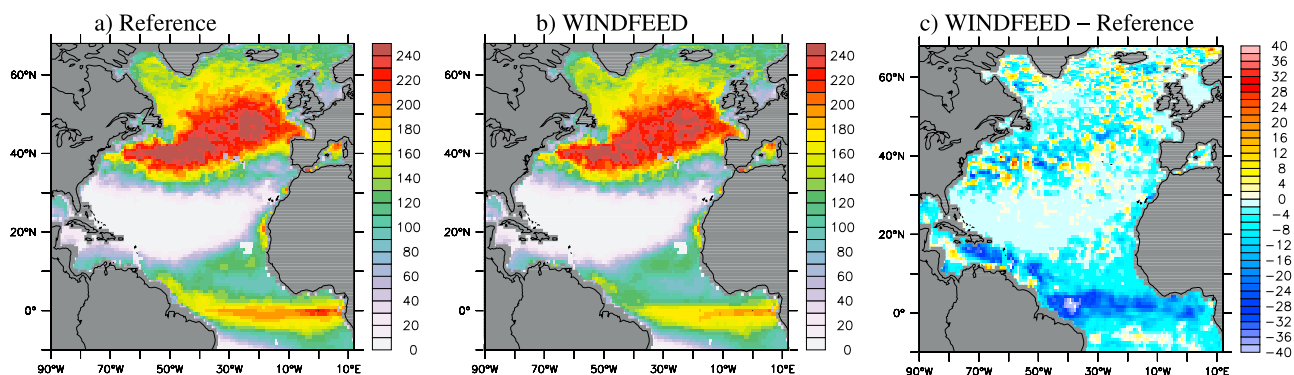


**Figure 8.** (a) Annual mean of vertically integrated carbon content in modeled phytoplankton standing stocks referring to year 2001 of the reference experiment. Units are  $\text{mmol C m}^{-2}$ . Data are box averaged over  $1^\circ \times 1^\circ$  prior to plotting. (b) Same as Figure 8a but for experiment WINDFEED. (c) Difference between Figures 8a and 8b, i.e., WINDFEED – reference experiment.

similar to other mesoscale eddy-permitting models [e.g., Oeschies, 2002b; McGillicuddy *et al.*, 2003].

[36] The difference in the phytoplankton concentration between both experiments are shown in Figure 8c. The overall pattern is a reduction of phytoplankton standing stocks induced by the feedback of ocean surface currents on the wind stress forcing the ocean. The largest reduction, exceeding  $40 \text{ mmol C m}^{-2}$  and corresponding to a relative decrease of about 20%, shows up in the western tropical Atlantic. The largest relative decrease in phytoplankton concentration, on the other hand, is along the southwesterly margin of the subtropical gyre, where the phytoplankton concentration is reduced by more than 100%. However, note that there, the concentrations are very small such that the absolute magnitude of the reduction is small and is hardly detectable in Figure 8.

[37] Within the NAC region, small mesoscale features with enhanced or reduced phytoplankton concentrations dominate. This is related to incoherent eddy activity within the two experiments since although both experiments share the same spin-up integration, the mesoscale eddy field in both experiments diverges in the beginning of the year 2001 and becomes incoherent after a couple of weeks because of

the difference in the forcing of the experiments. The effect is naturally most pronounced in regions of high eddy activity such as the Gulf Stream/NAC region and extends into the subsequent years of the simulation. Figure 9 shows the zonally integrated phytoplankton biomass for each year as well as the respective temporal averages over the 2001 to 2005 period as simulated by the two models. As most of the effect of the incoherent mesoscale features cancels out on a zonal average we conclude that there is, if at all, only a minor effect of the eddy-wind interaction on the phytoplankton stocks in midlatitudes. Differences in stocks between individual years in midlatitudes can be related to the interannual variability in the surface forcing, while the reduction of about 15% near the equator is persistent in each individual year and is therefore interpreted as a consequence of the revised wind stress parameterization in the experiment WINDFEED.

### 3.6. New Production and Air-Sea Carbon Fluxes

[38] A main aim of coupled ecosystem-ocean circulation modeling is to quantify the contribution of marine biota to air-sea fluxes of  $\text{CO}_2$  at present and, eventually, for future climate scenarios. In that respect biological production

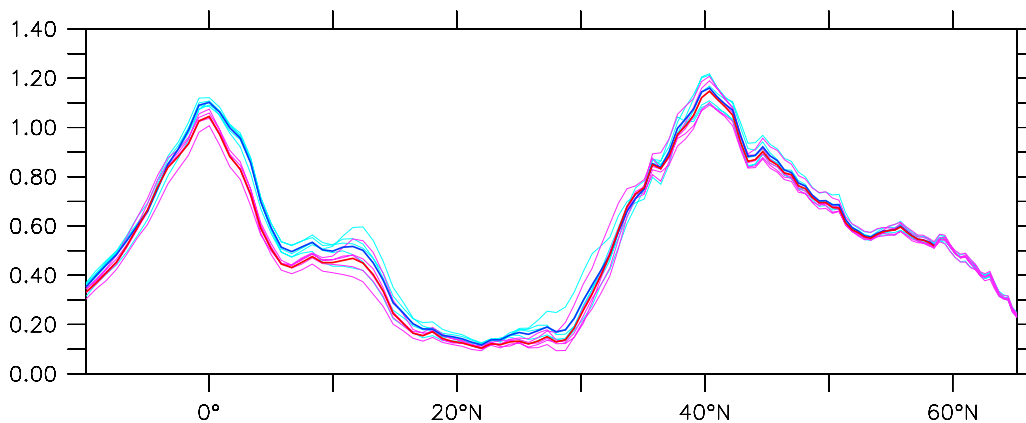


**Figure 9.** Temporal means of vertically and zonally integrated carbon content in modeled phytoplankton standing stocks in  $10^6 \text{ mol C m}^{-1}$ . Thin blue (red) lines refer to annual means covering the period from 2001 to 2005 from the reference experiment (WINDFEED). The bold blue (red) line denotes the average over the whole period in the reference experiment (WINDFEED).

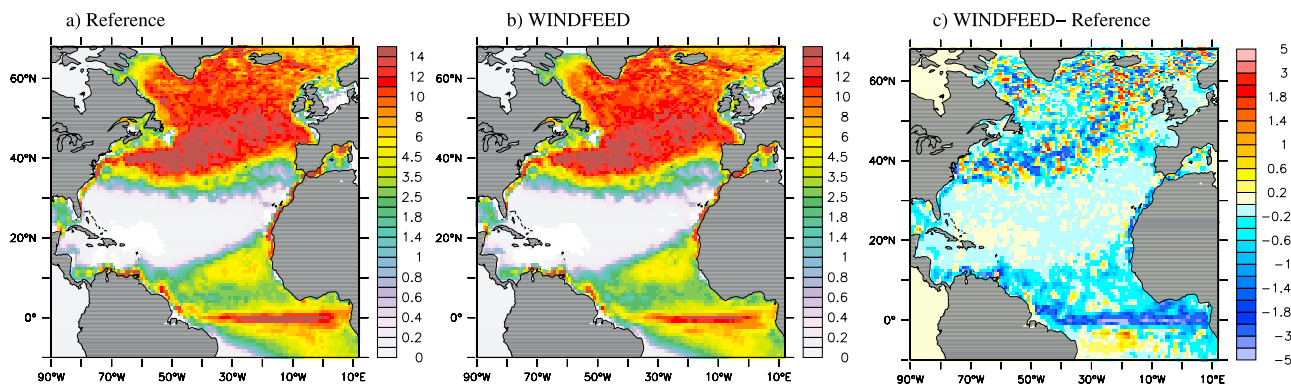


**Figure 10.** (a) Modeled new production integrated from the surface down to 120 m (in carbon units  $\text{mmol C m}^{-2} \text{d}^{-1}$ ) in the reference experiment. Data are box averaged over  $1^\circ \times 1^\circ$  prior to plotting. (b) Same as Figure 10a but for experiment WINDFEED. (c) Difference between Figures 10a and 10b, i.e., WINDFEED – reference experiment.

concepts such as new production, export production, and net community production are often applied since, even in models, it is not straight forward to disentangle biotically and physically induced air-sea gas fluxes [e.g., Jin *et al.*, 2007; Dietze and Oschlies, 2005]. Here, we use new production as a measure of the impact of marine biota on air-sea fluxes, although we are aware of the limitations of the concept as outlined by Oschlies and Kähler [2004]. Following Oschlies and Kähler [2004], we define the model equivalent of new production as the “total annual dissolved inorganic nitrogen supply into each grid-box column bounded by the sea surface and the maximum depth of the euphotic zone.” The maximum depth of the euphotic zone is set to 150 m. Furthermore, we assume a fixed C/N ratio to derive its carbon equivalent.

[39] The simulated new production which, in steady state, equals the export of organic material across the reference level of 150 m, is shown in Figure 10 for the year 2001 derived from WINDFEED and the reference experiment. In both experiments the regional distribution of the new production in the upper 150 m is similar to the distribution of the phytoplankton concentration, i.e., large, up to  $15 \text{ mmol m}^{-2} \text{d}^{-1}$  at maximum north of about  $35^\circ\text{N}$  and close to zero in the oligotrophic subtropical gyre of the North Atlantic. Toward the equator, the new production is increasing again and shows a second maximum at the equator with values similar to those modeled in the subpolar North Atlantic. Note that these estimates are within the envelope of variability in prior model studies [e.g., Oschlies, 2002b; McGillicuddy *et al.*, 2003]. Coherent differences between the two experiment are restricted to the equatorial region (Figure 10c), a fact that is mirrored in the zonal integrals of the period from 2001 to 2005 shown in Figure 11. The zonally integrated new production is, in general, reduced in WINDFEED compared to the reference experiment. In total we find a reduction of about 5% over the whole North Atlantic, but the difference between both experiments appears to be insignificant in midlatitudes, since there, interannual variability in new production is more dominant than the difference between both experiments for individual years (which does also apply for the phytoplankton standing stocks). On the other hand, at low latitudes, the decrease in new production due to

the revised parameterization of the wind stress is clearly significant, peaking at a reduction of 20% at the equator.

[40] The differences in zonally integrated air-sea fluxes of  $\text{CO}_2$  are even smaller than the differences in the export production of the two experiments (Figure 12a). This implies physical compensation by changes in solubility affected by heat fluxes and/or that new production is not necessarily a good measure for the biotic contribution to air-sea fluxes of  $\text{CO}_2$ . Here we only want to highlight that zonally integrated air-sea  $\text{CO}_2$  fluxes only differ significantly (i.e., more than their interannual variations) in the Gulf Stream/NAC region around  $40^\circ\text{N}$  where new production is similar in the two experiments. In fact, the enhanced oceanic heat losses in that region in the experiment WINDFEED relative to the reference (Figure 12b) implies that the increased oceanic  $\text{CO}_2$  uptake in the Gulf Stream/NAC region as modeled in WINDFEED is driven by physical rather than by biotic processes.

#### 4. Summary and Discussion

[41] We integrated a coupled ecosystem-ocean circulation model with mesoscale eddy-permitting resolution of the Atlantic Ocean, driven with high-resolution surface forcing from 2001 to 2006. In contrast to earlier studies [e.g., Oschlies, 2002b; McGillicuddy *et al.*, 2003], we applied a physically more plausible parameterization of the wind stress forcing. This revised parameterization takes into account that the wind stress is a function of the difference between atmospheric winds and surface ocean currents, rather than being a function of the atmospheric winds alone.

[42] The main changes in circulation associated with the revised parameterization are: First, an improved realism of the wind stress curl forcing the model when compared with satellite scatterometer data. Second, a reduction of the SEC; EUC; and, in particular (and noted already by Pacanowski [1987]), the equatorial upwelling. Third, a reduction of the near-surface eddy activity by about 10–20% in middle to high latitudes reproducing results from Duhaut and Straub [2006] and Zhai and Greatbatch [2007]. Furthermore, a significant damping of near-surface eddy activity in the tropical Atlantic, culminating at a reduction by 50% at the equator. The dominant mechanism behind this reduction of

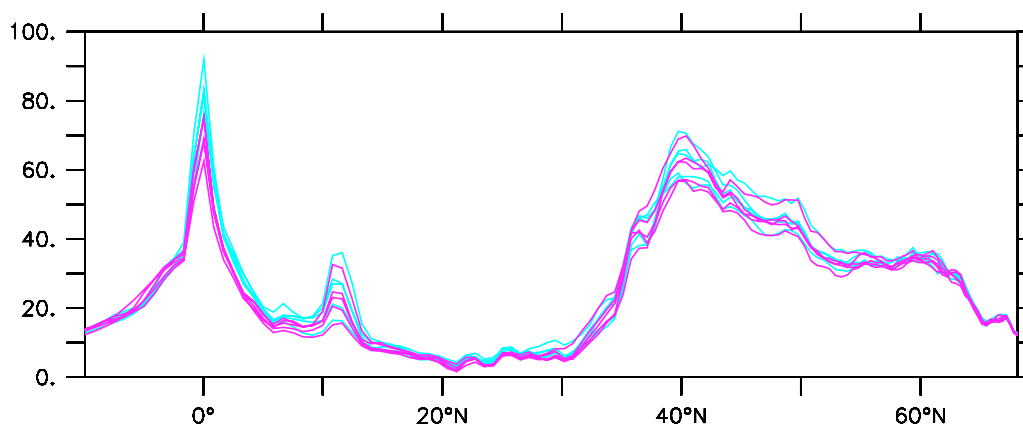


**Figure 11.** Modeled new production integrated vertically from the surface down to 120 m and zonally in carbon units ( $10^3 \text{ mol C m}^{-1} \text{ d}^{-1}$ ). Blue (red) lines refer to annual means of respective years in the 2001 to 2005 period calculated from the reference experiment (WINDFEED).

EKE was identified as the direct drag effect by the revised wind stress formulation with a minor, indirect, contribution from reduced near-surface EKE production by lateral shear instability. We speculate that the meridional gradient in the damping effect on EKE is a consequence of the correlated gradient in surface mixed layer depths, i.e., the drag effect on the eddy/wind interaction appears to be more important for the shallower mixed layer depths in the tropical Atlantic.

[43] Recently, *McGillicuddy et al.* [2007] and *Ledwell et al.* [2008] discussed the upwelling induced by eddy/wind interaction in an anticyclonic mode-water eddy and speculated that this effect might help to resolve an apparent, long-standing discrepancy between nutrient supply to [Lewis *et al.*, 1986] and oxygen consumption below [Jenkins, 1982] the euphotic zone of the subtropical gyre. Here we found that the overall effect of the revised wind stress formulation on basin-scale biotically affected carbon fluxes is rather low and in fact given by a modest reduction of export production of about 5% for the whole North Atlantic. Interannual variability of new production in the simulation was found to be larger than the effect of the revised wind stress formulation in the midlatitude to high-latitude North Atlantic. At the equator the reduction of new production was significant, its underlying mechanism identified as the reduced mean equatorial upwelling which comes along with less nutrients

supplied to the sunlit surface ocean, which in turn reduces associated vertical fluxes of organic matter (and phytoplankton standing stocks).

[44] Our results suggest that previous model estimates of export production in the subtropical gyre are not biased low because of the eddy/wind interaction. To the contrary, we find a decrease in new production by including the eddy/wind interaction in our model. It seems therefore unlikely that this effect helps to explain the apparent, long-standing discrepancy between nutrient supply to the euphotic zone of the subtropical gyre, as previously speculated.

[45] The results of the present study are in agreement with the findings of *Martin and Richards* [2001] and *Mahadevan et al.* [2008] insofar as they show that the eddy/wind interaction on biological production is small on the basin scale. On the other hand, *Martin and Richards* [2001] and *Mahadevan et al.* [2008] also argue that ageostrophic vertical velocities related to submesoscale eddy activity contribute significantly to biological production. However, we find in our model that the decrease in mesoscale eddy activity is not related to a correspondingly significant decrease in biological production. This finding is in agreement with previous observational estimates [Falkowski *et al.*, 1991] and realistic basin-scale model-based estimates [Oschlies, 2002a, 2008] which point to a mesoscale eddy-

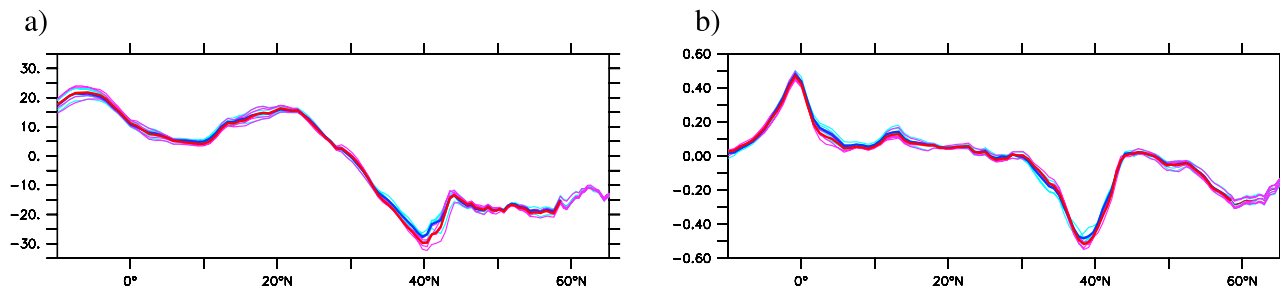


**Figure 12.** (a) Modeled zonally integrated air-sea  $\text{CO}_2$  exchange (including both the biotically and physically induced fraction) in  $10^3 \text{ mol C m}^{-1} \text{ d}^{-1}$ . Blue (red) lines refer to annual means of respective years in the 2001 to 2005 period calculated from the reference experiment (WINDFEED). Temporal means over the whole 2001 to 2005 period are drawn as bold blue and bold red lines, respectively. (b) Zonally averaged air-sea heat flux in  $10^9 \text{ W m}^{-1}$  in same color coding as in Figure 12a. Positive values denote flux from sea to air in both cases.

driven contribution of the upper ocean nutrient supply of less than 20% on the basin scale while the dominant nutrient supply is given by the mean flow. Since we use a prognostic ecosystem model very similar to the one in the papers by *Oschlies* [2002a, 2008] it is not surprising that a reduction of 10–20% of the eddy activity in midlatitudes causes only a small response in new production and carbon uptake in our simulations. To our knowledge, all models which suggest a stronger correlation between eddy activity and upper ocean nutrient supply recharge nutrients in the sub-euphotic zone by restoring to climatological nutrient fields [McGillicuddy and Robinson, 1997; McGillicuddy et al., 2003]. Note that *Oschlies* [2002a] and *Martin and Pondaven* [2003] argued that this class of models overestimates eddy-driven upper ocean nutrient supply, since the models with prognostic ecosystems extending down to the thermocline yield much lower values.

[46] **Acknowledgments.** This study was supported by the German DFG as part of the SFB 754. Suggestions and discussions with Andreas *Oschlies*, Anne-Marie Treguier, and Patrice Klein have been helpful and are appreciated. The model integrations have been performed on a NEX-SX8 at the University Kiel and on a NEC-SX6 at the Deutsches Klimarechenzentrum (DKRZ), Hamburg.

## References

- Andrews, D. G., J. R. Holton, and C. B. Leovy (1987), *Middle Atmosphere Dynamics*, 489 pp., Academic, San Diego, Calif.
- Barnier, B., L. Siefridt, and P. Marchesiello (1995), Thermal forcing for a global ocean circulation model using a three year climatology of ECMWF analysis, *J. Mar. Syst.*, **6**, 363–380.
- Beckmann, A., C. W. Böning, C. Köberle, and J. Willebrand (1994), Effects of increased horizontal resolution in a simulation of the North Atlantic Ocean, *J. Phys. Oceanogr.*, **24**, 326–344.
- Boyer, T. P., and S. Levitus (1997), *Objective Analyses of Temperature and Salinity for the World Ocean on a 1/4 Degree Grid*, NOAA Atlas NESDIS, vol. 11, NOAA, Silver Spring, Md.
- Capet, X., J. McWilliams, M. Molemaker, and A. Shchepetkin (2008), Mesoscale to submesoscale transition in the California Current System. Part I: Flow structure, eddy flux, and observational tests, *J. Phys. Oceanogr.*, **38**, 29–43.
- Dewar, W., and G. Flierl (1987), Some effects of the wind on rings, *J. Phys. Oceanogr.*, **17**, 1653–1667.
- Dietze, H., and A. *Oschlies* (2005), On the correlation between air-sea heat flux and abiotically induced oxygen gas exchange in a circulation model of the North Atlantic, *J. Geophys. Res.*, **110**, C09016, doi:10.1029/2004JC002453.
- Doney, S. C., D. Glover, S. McCue, and M. Fuentes (2003), Mesoscale variability of Sea-viewing Wide Field-of-view Sensor (SeaWiFS) satellite ocean color: Global patterns and spatial scales, *J. Geophys. Res.*, **108**(C2), 3024, doi:10.1029/2001JC000843.
- Duhaut, T. H. A., and D. N. Straub (2006), Wind stress dependence on ocean surface velocity: Implications for mechanical energy input to ocean circulation, *J. Phys. Oceanogr.*, **36**, 202–211.
- Eden, C. (2006), Mid-depth equatorial tracer tongues in a model of the Atlantic Ocean, *J. Geophys. Res.*, **111**, C12025, doi:10.1029/2006JC003565.
- Eden, C., and C. W. Böning (2002), Sources of eddy kinetic energy in the Labrador Sea, *J. Phys. Oceanogr.*, **32**, 3346–3363.
- Eden, C., and T. Jung (2006), Wind-driven eddies and plankton blooms in the North Atlantic Ocean, *Tech. Memo. 460*, Eur. Cent. for Medium-Range Weather Forecasts, Reading, U.K.
- Eden, C., and C. *Oschlies* (2006), Adiabatic reduction of circulation-related CO<sub>2</sub> air-sea flux biases in North Atlantic carbon-cycle models, *Global Biogeochem. Cycles*, **20**, GB2008, doi:10.1029/2005GB002521.
- Falkowski, P. G., D. Ziemann, Z. Kolber, and P. Bienfang (1991), Role of eddy pumping in enhancing primary production in the ocean, *Nature*, **352**, 55–58.
- Gaspar, P., Y. Gregoris, and J.-M. Lefevre (1990), A simple eddy kinetic energy model for simulations of the oceanic vertical mixing: Tests at station PAPA and Long-Term Upper Ocean Study site, *J. Geophys. Res.*, **95**, 16,179–16,193.
- Gent, P. R., and J. C. McWilliams (1990), Isopycnal mixing in ocean circulation models, *J. Phys. Oceanogr.*, **20**, 150–155.
- Giordani, H., L. Prieur, and G. Caniaux (2006), Advanced insights into sources of vertical velocity in the ocean, *Ocean Dyn.*, **56**(5), 513–524.
- Haine, T., and J. Marshall (1998), Gravitational, symmetric and baroclinic instability of the ocean mixed layer, *J. Phys. Oceanogr.*, **28**, 634–658.
- Jenkins, W. J. (1982), Oxygen utilization rates in the North Atlantic subtropical gyre and primary production in oligotrophic systems, *Nature*, **300**, 246–248.
- Jenkins, W. J. (1988), Nitrate fluxes into the euphotic zone near Bermuda, *Nature*, **331**, 521–523.
- Jerlov, N. G. (1976), *Marine Optics*, Elsevier, New York.
- Jin, X., R. G. Najjar, F. Louanchi, and S. C. Doney (2007), A modeling study of the seasonal oxygen budget of the global ocean, *J. Geophys. Res.*, **112**, C05017, doi:10.1029/2006JC003731.
- Large, W. G., and S. G. Yeager (2004), Diurnal to decadal global forcing for ocean and sea-ice models: The data sets and flux climatologies, Rep. NCAR/TN-460+STR, 105 pp., Natl. Cent. for Atmos. Res., Boulder, Colo.
- Ledwell, J. R., D. J. McGillicuddy, and L. A. Anderson (2008), Nutrient flux into an intense deep chlorophyll layer in a mode-water eddy, *Deep Sea Res., Part II*, **55**, 1139–1160, doi:10.1016/j.dsr2.2008.02.005.
- Legal, C., P. Klein, A. Treguier, and J. Paillet (2007), Diagnosis of the vertical motions in a mesoscale stirring region, *J. Phys. Oceanogr.*, **37**, 1413–1424.
- Levitus, S., and T. P. Boyer (1994), *World Ocean Atlas 1994*, vol. 4, *Temperature*, NOAA Atlas NESDIS, vol. 4, 129 pp., NOAA, Silver Spring, Md.
- Lévy, M. (2003), Mesoscale variability of phytoplankton and of new production: Impact of the large-scale nutrient distribution, *J. Geophys. Res.*, **108**(C11), 3358, doi:10.1029/2002JC001577.
- Lévy, M., P. Klein, and A. Treguier (2001), Impact of sub-mesoscale physics on production and subduction of phytoplankton in an oligotrophic regime, *J. Mar. Res.*, **59**, 535–565.
- Lewis, M. R., W. G. Harrison, N. S. Oakey, D. Herbert, and T. Platt (1986), Vertical nitrate fluxes in the oligotrophic ocean, *Science*, **234**, 870–873.
- Mahadevan, A., and D. Archer (2000), Modeling the impact of fronts and mesoscale circulation on the nutrient supply and biogeochemistry of the upper ocean, *J. Geophys. Res.*, **105**, 1209–1225.
- Mahadevan, A., and A. Tandon (2006), An analysis of mechanisms for submesoscale vertical motion at ocean fronts, *Ocean Modell.*, **14**, 241–256.
- Mahadevan, A., L. Thomas, and A. Tandon (2008), Comment on “Eddy/wind interactions stimulate extraordinary mid-ocean plankton blooms,” *Science*, **320**, 448.
- Martin, A., and P. Pondaven (2003), On estimates for the vertical nitrate flux due to eddy pumping, *J. Geophys. Res.*, **108**(C11), 3359, doi:10.1029/2003JC001841.
- Martin, A., and K. Richards (2001), Mechanisms for vertical nutrient transport within a North Atlantic mesoscale eddy, *Deep Sea Res., Part II*, **48**, 757–773.
- Martin, A. P., K. J. Richards, and M. J. R. Fasham (2001), Phytoplankton production and community structure in an unstable frontal region, *J. Mar. Syst.*, **28**, 65–89.
- McGillicuddy, D. J. J., and A. R. Robinson (1997), Eddy-induced nutrient supply and new production in the Sargasso Sea, *Deep Sea Res., Part I*, **44**, 1427–1450.
- McGillicuddy, D. J., L. A. Anderson, S. C. Doney, and M. E. Maltrud (2003), Eddy-driven sources and sinks of nutrients in the upper ocean: Results from a 0.1° resolution model of the North Atlantic, *Global Biogeochem. Cycles*, **17**(2), 1035, doi:10.1029/2002GB001987.
- McGillicuddy, D. J., et al. (2007), Eddy/wind interactions stimulate extraordinary mid-ocean plankton blooms, *Science*, **316**, 1021–1026, doi:10.1126/science.1136256.
- Olson, D. (1986), Lateral exchange within Gulf Stream warm-core ring surface layers, *Deep Sea Res., Part A*, **33**, 1691–1704.
- Oschlies*, A. (2002a), Improved representation of upper ocean dynamics and mixed layer depths in a model of the North Atlantic on switching from eddy-permitting to eddy-resolving grid resolution, *J. Phys. Oceanogr.*, **32**, 2277–2298.
- Oschlies*, A. (2002b), Can eddies make ocean deserts bloom?, *Global Biogeochem. Cycles*, **16**(4), 1106, doi:10.1029/2001GB001830.
- Oschlies*, A. (2008), Eddies and upper-ocean nutrient supply, in *Ocean Modeling in an Eddying Regime*, *Geophys. Monogr. Ser.*, vol. 177, edited by M. Hecht and H. Hasumi, pp. 115–130, AGU, Washington, D. C.
- Oschlies*, A., and V. Garçon (1998), Eddy induced enhancement of primary production in a model of the North Atlantic Ocean, *Nature*, **394**, 266–269.
- Oschlies*, A., and P. Kähler (2004), Biotic contribution to air-sea fluxes of CO<sub>2</sub> and O<sub>2</sub> and its relation to new production, export production, and net community production, *Global Biogeochem. Cycles*, **18**, GB1015, doi:10.1029/2003GB002094.

- Pacanowski, R. (1987), Effect of equatorial currents on surface stress, *J. Phys. Oceanogr.*, *17*, 833–838.
- Paulson, C., and J. Simpson (1977), Irradiance measurements in the upper ocean, *J. Phys. Oceanogr.*, *7*, 952–956.
- Smith, R. D., M. E. Maltrud, F. O. Bryan, and M. W. Hecht (2000), Numerical simulation of the North Atlantic Ocean at  $1/10^\circ$ , *J. Phys. Oceanogr.*, *30*, 1532–1561.
- Stevens, D. P. (1990), On open boundary conditions for three dimensional primitive equation ocean circulation models, *Geophys. Astrophys. Fluid Dyn.*, *51*, 103–133.
- Tilburg, C., B. Subrahmanyam, and J. O'Brien (2002), Ocean color variability in the Tasman Sea, *Geophys. Res. Lett.*, *29*(10), 1487, doi:10.1029/2001GL014071.
- Xu, Y., and R. B. Scott (2008), Subtleties in forcing eddy resolving ocean models with satellite wind data, *Ocean Modell.*, *20*, 240–251.
- Zhai, X., and R. Greatbatch (2007), Wind work in a model of the northwest Atlantic Ocean, *Geophys. Res. Lett.*, *34*, L04606, doi:10.1029/2006GL028907.

---

H. Dietze and C. Eden (corresponding author), IFM-GEOMAR, Düsternbrooker Weg 20, D-24105 Kiel, Germany. (ceden@ifm-geomar.de)